# SCIENCE CHINA

# Information Sciences

• RESEARCH PAPER •

January 2015, Vol. 58 012202:1–012202:21 doi: 10.1007/s11432-014-5179-4

# Characteristic model-based $H_2/H_\infty$ robust adaptive control during the re-entry of hypersonic cruise vehicles

HUANG Huang<sup>1,2</sup>\* & ZHANG Zhao<sup>1,2</sup>

<sup>1</sup>Beijing Institute of Control Engineering, Beijing 100190, China; <sup>2</sup>Science and Technology on Space Intelligent Control Laboratory, Beijing 100190, China

Received April 1, 2014; accepted July 8, 2014; published online September 15, 2014

Abstract This paper aims at introducing  $H_2$  and  $H_\infty$  robustness into the well-known characteristic model-based golden-section adaptive control law, and applying the robust adaptive control scheme to the attitude control of hypersonic cruise vehicles that are subject to external disturbances and aerodynamic coefficients uncertainties. When maneuvering at ultra high speeds, the attitude system of the hypersonic cruise vehicle is extremely sensitive to external disturbances and aerodynamic coefficients variations, and therefore the adaptiveness and the robustness of the attitude system are crucial during the controller design. To enhance the robustness of the existing golden-section adaptive control law, a golden-section robust adaptive control law is proposed. Compared to the existing control law where the design of the parameter  $\lambda$  depends on experience and is carried out offline, linear matrix inequality-based synthesis of  $\lambda$  is proposed such that the closed-loop system is stable with guaranteed  $H_2$  and  $H_\infty$  performance. It is suitable for online computing and provides a time-varying  $\lambda(k)$  that is adjusted towards the optimal  $H_2$  and  $H_\infty$  performance. When being applied to the attitude control of hypersonic vehicles during re-entry, the adaptive nature of the proposed control law provides the attitude system the capability to accommodate large flight conditions, and its  $H_2$  and  $H_\infty$  robustness brought by  $\lambda(k)$  guarantees satisfying tracking performance in the presence of disturbances including both external disturbance and absolute aerodynamic coefficients errors.

**Keywords** golden-section adaptive control, characteristic model,  $H_2$  and  $H_\infty$  analysis, hypersonic vehicle, attitude control

Citation Huang H, Zhang Z. Characteristic model-based  $H_2/H_{\infty}$  robust adaptive control during the re-entry of hypersonic cruise vehicles. Sci China Inf Sci, 2015, 58: 012202(21), doi: 10.1007/s11432-014-5179-4

# 1 Introduction

Research on hypersonic cruise vehicles could be dated back to 1963 characterized by the first successful flight of X-15 hypersonic vehicle at Mach 6.7 and an altitude of 12 km. Over the last decades, numerous scientists and engineers have contributed themselves into this challenging field. The successful flight experiments of the scramjet-powered hypersonic cruise vehicle X-43A in 2004 at Mach 7 and Mach 10 are an inspiring step into the future [1]. Prominent features of hypersonic cruise vehicles include (1) short

<sup>\*</sup>Corresponding author (email: hhuang33@gmail.com)

developing cycle, (2) global reach within 2 hours, and (3) affordable and reliable access to space, all of which have both commercial and military implications. However, these features are accompanied by tremendous challenges where one of the most critical issues is the attitude control [2,3].

The attitude dynamics of hypersonic cruise vehicles are generally depicted by a 6-DOF nonlinear model with strong couplings between variables. A significant amount of literatures has been devoted to the attitude control of hypersonic vehicles from various perspectives. When treating the nonlinear model directly, the adaptive control [4,5], the robust control [6,7], and the sliding mode control [8] are some of the most popular methods. The dynamic inversion control, which provides an effective way to overcome the nonlinearity of the system, has also been investigated in quite a few literatures [9–11]. Because of the slowly varying nature during the gliding phase, linearization is carried out at several trim conditions. To improve the dynamic performance, the switching among different controllers is based on the gain-scheduling technique [12]. Other methods such as the tangent linearization control [13] over the flight envelope, and very recently, the support vector regression-based method [14], have also showed their potentials. Combinations of several methodologies provide satisfying performance as well [15].

As can be seen, research on hypersonic cruise vehicles has experienced blooming development over the past few years. However, the well-known hypersonic cruise vehicle HTV-2 (belongs to the DARPA/Air Force Falcon Technology Programme) underwent two subsequent failures in 2010 and 2011. Flying at a velocity of up to Mach 20, this program propels the exploration of hypersonic vehicles into the next era, and however again, reminds us of the rough road to go.

Compared to aircrafts operating within the conventional speed range, hypersonic cruise vehicles flying at a speed above Mach 5, or even cruising at Mach 20, will experience ultra high dynamic pressure, which, together with its intrinsic configuration, will further result in an extremely vulnerable or sensitive system in the presence of aerodynamic coefficients uncertainties and external disturbances. Because of the limited flight experiments and inadequate ground test facilities, aerodynamic coefficients uncertainties also show serious deviations in both an absolute manner and a relative manner, which brought huge challenges in controller design. Most literatures concerning parameter uncertainties are restricted to relative errors, as, for example, in [6,16]. In [16], aerodynamic uncertainties were overcome by adding an adaptive component to the baseline controller. Similar to many other literatures, the controller design is based on the linearized model that is obtained at several trim conditions. However, in the presence of absolute errors, there may exist an excursion on the trim condition that affects the corresponding linearized model, and consequently the stability of the closed-loop system. Only a limited number of literatures has included both the two types of uncertainties, as in [14]. According to our previous work, aerodynamic coefficients uncertainties, the absolute offsets in particular, are fatal to the stability of the attitude system. This phenomenon becomes more prominent when vehicle maneuvers at high Mach numbers and in relatively dense atmosphere. This observation motivates the present study.

On the other hand, the well-known characteristic model, which was proposed in the 1990s by Wu, has been developed for more than 20 years and accommodated by the golden-section adaptive control law [17,18]. The essence of the characteristic model is to use a low-order discrete time-varying system to approach a high-order nonlinear or linear system based on the characteristics of the plant and control performance requirements. Rather than dropping information as in reduced-order modeling, it compresses/integrates all the information of the high-order model into several characteristic parameters. Based on this characteristic model, golden-section adaptive control law was further proposed with the prominent features including both easy implementation and guaranteed stability during the parameter convergence, as compared with other adaptive control laws. The characteristic model theory has bred a few inspiring methodologies. In [19,20], fuzzy model and the characteristic model were combined into the fuzzy dynamic characteristic model, which inherits the advantages of online adaption and easy implementation that are brought by characteristic model, and more precise modeling that is brought by the fuzzy model. The characteristic model was also introduced into the model predictive control so as to avoid model mismatching [21]. This control scheme has already been applied to more than 400 systems belonging to 10 kinds of engineering plants in the fields of astronautics (such as in the rendezvous and docking of Shenzhou-8 spacecraft [22]) and industry [17,23]. In recent years, its potential in hypersonic vehicle control was explored during both cruising phase [20,24] and climbing phase [25].

To this end, towards the nonlinearity of the attitude dynamics during the re-entry phase, this paper introduces the characteristic model to provide a control-oriented model where the characteristic parameters are identified online so as to suit the changing environment and flight status. Golden-section adaptive control law is designed for stable tracking of the commanded angles. The absolute parameter uncertainties are treated as an external disturbance to the system, and thus  $H_2/H_\infty$  robustness is incorporated into the existing golden-section adaptive control law through its parameter  $\lambda(k)$  at each sampling time. Because of the non-uniqueness of  $\lambda(k)$ , LMI-based criterions are proposed that provide an effective way to adjust the parameter  $\lambda$  rather than tuning it according to the designer's experience. When applying the robust adaptive control scheme to hypersonic cruise vehicles during re-entry, in the large time scale, it depends on the adaption of the characteristic parameters to restrain the states near the commanded value, and during each sampling interval, it relies on  $\lambda(k)$ , in particular, to compensate the influences brought by absolute parameter uncertainties and external disturbances. This control scheme integrates the adaptive control and the robust control in a cooperative way.

The rest of the paper is organized as follows. Section 2 introduces the backgrounds on the characteristic model, and builds the characteristic model of the hypersonic cruise vehicle. Section 3 discusses the existence of the coefficient  $\lambda$  in the golden-section adaptive control law, and further explores the synthesis of  $\lambda(k)$  that improves the  $H_2/H_{\infty}$  robustness based on the state feedback control and the output feedback control, respectively. Section 4 demonstrates the effectiveness and the prominent features of the proposed control scheme through the hypersonic attitude control. Conclusion is provided in Section 5.

## 2 Characteristic modeling of hypersonic cruise vehicles

### 2.1 The characteristic model and the golden-section adaptive control law

Let  $\mathbb{R}$  be the set of real numbers. The  $L_2$  norm and the  $L_\infty$  norm of a signal  $x(k) \in \mathbb{R}^n, k = 0, 1, 2, \ldots$  are  $\|x(k)\|_2 = \left(\sum_{k=0}^\infty \|x(k)\|^2\right)^{1/2}$  and  $\|x(k)\|_\infty = \sup_{k\geqslant 0} \|x(k)\|$ , respectively, where  $\|x(k)\| = \sqrt{x^{\mathrm{T}}(k)x(k)}$  is the Euclidian norm of the vector.

In the following context, the characteristic model and the golden-section adaptive control law are introduced. The related existing results inherited from [17,18,24,26,27] are presented in the lemmas and remarks.

The general transformation function for a single-input-single-output (SISO) linear time invariant system is

$$G(s) = \frac{b_m s^m + b_{m-1} s^{m-1} + \dots + b_1 s + b_0}{s^n + a_{n-1} s^{n-1} + \dots + a_1 s + a_0},$$
(1)

where  $m \leq n$  are positive integers and  $a_i, b_i \in \mathbb{R}, b_m \neq 0$ .

If G(s) in (1) has  $\gamma_1$  zero eigenvalues,  $\gamma_2$  non-zero real eigenvalues  $\lambda_i$ ,  $i = 1, ..., \gamma_2$ , and  $\gamma_3$  pairs of complex eigenvalues  $\alpha_i + i\beta_i$ ,  $i = 1, ..., \gamma_3$ , its decomposed form is then

$$G(s) = \sum_{i=1}^{\gamma_1} \frac{l_i}{s^i} + \sum_{i=1}^{\gamma_2} \sum_{j=1}^{\nu_i} \frac{r_{ij}}{(s - \lambda_i)^j} + \sum_{i=1}^{\gamma_3} \sum_{j=1}^{\nu_i} \frac{p_{ij}s + q_{ij}}{((s - \alpha_i)^2 + \beta_i^2)^j}.$$

For the discretization of continuous system G(s), the following assumption on the sampling time  $\Delta_t$  is made:

#### Assumption 1.

$$\Delta_t \ll \min\{|\underline{\lambda}|, |\bar{\lambda}|, \max_{i=1,\dots,\gamma_3} (\pi/\beta_i, \epsilon/M)\},$$

where  $\epsilon$  is sufficiently small, M is the upper bound of  $|\dot{y}(t)|, y = G(s)u$ , and

$$\underline{\lambda}(\bar{\lambda}) = \min(\max) \left\{ \lambda_1, \dots, \lambda_{\gamma_2}, \alpha_1 + \frac{\beta_1^2}{\alpha_1}, \dots, \alpha_{\gamma_3} + \frac{\beta_{\gamma_3}^2}{\alpha_{\gamma_3}} \right\}.$$

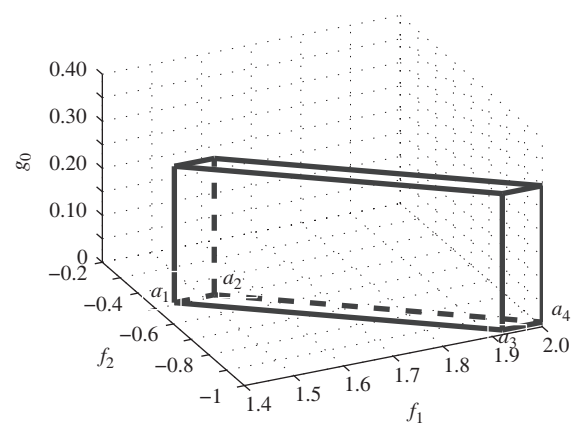


Figure 1 The three variables lie in a prism.

The characteristic model for the linear system G(s) is then

**Lemma 1** ([18]). Consider a linear time invariant system G(s) under Assumption 1, if G(s) has no eigenvalues on the imaginary axis, and when the control requirement is position keeping or tracking, its characteristic model has the following second-order difference form:

$$y(k+1) = f_1(k)y(k) + f_2(k)y(k-1) + g_0(k)u(k),$$
(2)

where  $g_0(k) = O(\Delta_t)$  and

$$f_1(k) \in \begin{cases} [2, 2 + 2\Delta_t \overline{\lambda}], & \overline{\lambda} > \underline{\lambda} > 0, \\ [2 + 2\Delta_t \underline{\lambda}, 2], & \underline{\lambda} < \overline{\lambda} < 0, \\ 2 + 2\Delta_t [\underline{\lambda}, \overline{\lambda}], & \text{Otherwise,} \end{cases} f_2(k) \in \begin{cases} [-(1 + 2\Delta_t \overline{\lambda}), -1], & \overline{\lambda} > \underline{\lambda} > 0, \\ [-1, -(1 + 2\Delta_t \underline{\lambda})], & \underline{\lambda} < \overline{\lambda} < 0, \\ -1 - 2\Delta_t [\overline{\lambda}, \underline{\lambda}], & \text{Otherwise.} \end{cases}$$

**Remark 1.** To improve the transient performance of the closed-loop system, there is sometimes an additional factor  $g_1(k)u(k-1)$  being added to y(k+1). In engineering applications, when treating a minimal phase system or a weakly non-minimal phase system, this factor is always omitted for simplicity [27]. Thus, the characteristic model (2) is more commonly used rather than the one discussed in [18].

The parameters  $f_i$  and  $g_i$  in the characteristic model are identified online based on the least square method or the gradient method [28]. Let  $\hat{f}_i$  and  $\hat{g}_i$  be the estimations of  $f_i$  and  $g_i$ , respectively. The triplets  $\Gamma = [f_1, f_2, g_0]$  and  $\hat{\Gamma} = [\hat{f}_1, \hat{f}_2, \hat{g}_0]$  belong to a prism whose eight vertexes are denoted by  $\bar{\Gamma} = [\bar{f}_{1i}, \bar{f}_{2i}, \bar{g}_{0i}], i = 1, 2, \dots, 8$ . The prism is determined according to the sampling time and the layouts of the open-loop eigenvalues, that is,  $\Delta_t$ ,  $\bar{\lambda}$ , and  $\underline{\lambda}$ . When  $\Delta_t$  is relatively large, the bound is comparatively loose. For a second-order system when  $\Delta_t/T_s = 1/3$  with  $T_s$  being the minimal equivalent time constant, the transverse section of the prism is a diamond, as for example shown in Figure 1. According to the layouts of the pair of eigenvalues in the continuous domain, the loose bounds, or the convex sets where the characteristic parameters belong to have three different cases (please refer to Chapter 5 in [27] for details).

When the estimations  $\hat{f}_i$  and  $\hat{g}_0$  are confined within the given convex hull, the corresponding estimated output  $\hat{y}(k)$  is such that

**Remark 2.** The transient estimation error  $\delta y(k) = \hat{y}(k) - y(k)$  is  $O(\Delta_t)$ , and the steady modeling error is zero.

Lemma 2. The system (2) in Lemma 1 is stable under the golden-section adaptive control law

$$u(k) = \frac{-[l_1\hat{f}_1(k)y(k) + l_2\hat{f}_2(k)y(k-1)]}{\lambda + \hat{g}_0(k)},$$
(3)

## 2.2 Characteristic modeling of the longitudinal dynamics

In addition to the high-order LTI system, it has further been proved that with an appropriate sampling time, the characteristic model (2) and the control law (3) also apply to the linear time-varying system and nonlinear system [27], including the attitude dynamics of hypersonic vehicles [24,25].

We consider hypersonic vehicles that maneuver with the engine off during the re-entry, and focus on the gliding and the terminal area energy management (TAEM) phase. In such a case, the hypersonic vehicle is subject to only aerodynamic force and gravity. Thus, its dynamics equation in the longitudinal plane proposed by Bolender et al. [29] has the simple form of

$$\dot{V} = -\frac{1}{m}D - g\sin\gamma, \quad \dot{r} = V\sin\gamma, \quad \dot{\gamma} = \frac{1}{mV}L - \left(\frac{V}{r} - \frac{g}{V}\right)\cos\gamma, \quad \dot{\alpha} = q - \dot{\gamma}, \quad \dot{q} = \frac{M_y(\alpha, \delta_e)}{I_y}, \quad (4)$$

where V, r,  $\gamma$ ,  $\alpha$ , q, m,  $M_y$ ,  $I_y$ , D, L, g, and  $\delta_e$  are the vehicle velocity, the radial distance from the Earth's center, the flight path angle, the angle of attack (AOA), the pitch rate, the vehicle mass, the pitching moment, vehicle y-axis inertia per unit width, the drag, the lift, the gravity acceleration, and the pitching control surface deflection, respectively. Note that the thrust T is omitted as the hypersonic vehicle we considered here is a glider that depends on the high lift-to-drag ratio for long-range gliding rather than a scram-jet powered engine.

When concentrating on the attitude dynamics, variables V and r are generally considered as slow modes, compared to fast modes  $\alpha$  and  $\delta_e$ , and thus are treated as constant values. Meanwhile, the lift force and the drag force are calculated according to  $L = \bar{q}SC_L$  and  $D = \bar{q}SC_D$ , where  $\bar{q} = 1/2\rho V^2$  is the dynamic pressure and  $\rho$  is the air density. The lift and drag coefficients  $C_L$  and  $C_D$  are approximated by fitting the experimental data with second-order polynomials, such as the one in [30], where  $C_L$  and  $C_D$  are not sensitive to AOA or  $M_V$ . In other words, when concentrating on the dynamics of  $\alpha$ , the lift L and drag D could be taken constant as well.

The dynamics of the AOA has a relative degree of 2 [24]. Thus its second-order differential equation derived from (4) is

$$\ddot{\alpha} = \dot{q} - \ddot{\gamma} = \frac{1/2\bar{q}S_{\text{ref}}l_{\text{ref}}C_{\text{my}}(\alpha, \delta_e)}{I_y} - \frac{gr - V^2}{Vr}\dot{\gamma}\sin\gamma \approx \frac{1/2\bar{q}S_{\text{ref}}l_{\text{ref}}C_{\text{my}}(\alpha, \delta_e)}{I_y} \triangleq f(\alpha, \delta_e),$$
 (5)

where  $S_{\rm ref}$  and  $l_{\rm ref}$  are the reference area and reference length, respectively, and the aerodynamic coefficients  $C_{\rm my}$  in the longitudinal plane is obtained by the linear interpolation method. Note that for vehicles flying at Mach 5 and above, the first item in (5) is generally greater than 0.1, while the second item  $\frac{gr-V^2}{Vr}\dot{\gamma}\sin\gamma$  belongs to  $10^{-4}$ . Thus, the second item could be omitted during the abbreviation for simplicity.

The nonlinear function  $f(\alpha, \delta_e)$  is such that

- (i)  $|f(\alpha(t+\Delta t), \delta_e(t+\Delta t))| |f(\alpha(t), \delta_e(t))| < M\Delta t, M > 0;$
- (ii) the partial differentials of  $f(\alpha, \delta_e)$  on  $\alpha$  and  $\delta_e$  are bounded;
- (iii) f(0,0) = 0.

According to the characteristic model in Section 2, with an appropriate sampling time  $\Delta_t$  and when the control requirement is angle keeping or tracking, the characteristic model for the angle of attack  $\alpha$  in (5) is

$$\alpha(k+1) = f_1(k)\alpha(k) + f_2(k)\alpha(k-1) + g_0(k)\delta_e(k).$$
(6)

Similar analysis and the second-order characteristic model apply to the roll angle and the sideslip angle as well.

### 3 Golden-section robust adaptive control law

During the re-entry of the hypersonic vehicle, its ultra high speed and its intrinsic configuration produce an extremely sensitive attitude system. Measurements on the aerodynamic coefficients become inadequate and are beyond the capability of ground wind tunnels test. Small aerodynamic coefficients uncertainties, the absolute uncertainties in particular, may drag the trim conditions away from the designed ones such that controllers that are designed for the linearized models are no longer reliable, and hence jeopardize the stability. Although the attitude system is stable, its transient performance may not be maintained in a satisfying level.

Although both the absolute offset and the relative offset are caused by disturbances to the aerodynamic coefficients, the relative error only affects the nonzero coefficients, while the absolute error further affects the zero coefficients. For example, in the nominal case when the elevon deflection is zero, that is,  $\delta_e = 0$ , the corresponding pitching moment coefficient  $C_{\rm my0} = 0$ , which means it has no control effort on the angle of attack. When absolute error  $\Delta C_{\rm my} \neq 0$ , the new pitching moment coefficient is  $C_{\rm my} = C_{\rm my0} + \Delta C_{\rm my} \neq 0$ , that is, elevon on its zero position will now produce a pitching moment that affects the angle of attack. In the presence of absolute error, this phenomenon becomes more prominent on the sideslip channel where the rudder may expect a nonzero deflection so as to overcome the unexpected yaw moment at zero sideslip angle.

Although the absolute offset could not be explicitly depicted by the standard characteristic model (6), it is in the essence a norm-bounded external disturbance that could be merged into the characteristic model (6) in the form of

$$\alpha(k+1) = f_1(k)\alpha(k) + f_2(k)\alpha(k-1) + g_0(k)\delta_e(k) + B_1(k)w(k), \tag{7}$$

where the absolute offset  $\delta_{abs}$  of the aerodynamic coefficients is incorporated into w(k) and its relative offset  $\delta_{rel}$  is accommodated by purely the adaption of the characteristic parameters.

By treating the absolute errors as external disturbances, the robustness of the system in the presence of exogenous disturbances should be strengthened during controller design so as to cope with the excursion of the trim conditions. In the presence of various uncertainties and disturbances,  $H_2$  and  $H_\infty$  performances are two of the most important robustness criterions that are used to evaluate the ability to resist exogenous disturbances.

The mixed  $H_2/H_{\infty}$  robust control problem has been discussed in numerous literatures concerning either the topic of cost-guaranteed filtering problem with state-error variance constraints [31], or the topic of robust controller design [32] even in a decentralized scheme [33]. When dealing with time-varying systems, gain-scheduled  $H_2/H_{\infty}$  control has been proved efficient to engineering problems [34]. However, the design of the conventional  $H_2$  and/or  $H_{\infty}$  controllers relies strongly on the system model, which itself is a crucial issue to the research of hypersonic vehicles. A common way is to use the linear model obtained at the trim condition. Because of the severe parametric uncertainties and aerodynamic changes [35,36], a large amount of trim conditions are expected so as to deal with the wide range of flight conditions during the re-entry phase, especially at low altitudes. In comparison with the constant controller, adaptive control that adjusts its parameters online is a more rational way for the attitude control during the entire re-entry phase. Thus, to fit the large flight conditions and to improve the transient performance in the presence of uncertainties and disturbances, the combined scheme of mixed  $H_2/H_{\infty}$  robustness and the golden-section adaptive control for hypersonic vehicles has a strong demand in practical applications.

Based on the conventional golden-section control law (3), a more intelligent golden-section adaptive control law is proposed with a time-varying  $\lambda(k)$ :

$$u(k) = \frac{-[l_1\hat{f}_1(k)y(k) + l_2\hat{f}_2(k)y(k-1)]}{\lambda(k) + \hat{g}_0(k)}.$$
 (8)

In the rest of the paper, the main focus is on seeking an effective and efficient way to determine  $\lambda(k)$  online, as compared with choosing a constant  $\lambda$  offline according to experience.

**Problem 1.** Find  $\lambda(k)$  such that system (2) under controller (8) is stable and, for all admissible exogenous disturbance w(k), criterions (i) and (ii) are satisfied:

(i) the  $H_{\infty}$  gain of the transfer function  $T_{z_{\infty}w}$  from w(k) to the corresponding outputs  $z_{\infty}(k)$  satisfies

$$J_{\infty} = \|T_{z_{\infty}w}\|_{\infty} < \gamma; \tag{9}$$

(ii) the  $H_2$  gain of the transfer function  $T_{z_2w}$  from w(k) to the corresponding outputs  $z_2(k)$  is guaranteed by

$$J_2 = ||T_{z_2w}||_2 \leqslant \bar{J}, \quad \bar{J} \in \mathbb{R}^+, \tag{10}$$

where  $\bar{J}$  is the upper bound of the  $H_2$  gain in the worst case.

The golden-section adaptive control law (8) with  $\lambda(k)$  satisfying the above criterions is then called a golden-section robust adaptive control law.

### 3.1 The existence of $\lambda(\mathbf{k})$

It has been proved in [26] that for a second-order time-invariant system whose characteristic model is a minimum phase one, the parameter  $\lambda$  in (3) equals zero, and when it is a non-minimum phase system but is stable in the open loop, there always exists  $\lambda > 0$  such that u(k) in (3) is a stable robust controller. Recently, it has further been proved through the root locus analysis that when the sampling time is small enough, there always exist  $\lambda$ , not necessarily being positive, such that the closed-loop system is stable [37]. These results were concluded according to the classical root locus analysis, and thus are limited to low-order systems. In this section, we further prove the existence of  $\lambda$  from the matrix perturbation theory perspective, which is ready to be extended to characteristic model of high orders.

At time instance k, the closed-loop system matrix of model (2) with controller (3) is

$$A_c = \begin{bmatrix} 0 & 1\\ f_2 - l_2 \frac{g_0}{\hat{g}_0 + \lambda} \hat{f}_2 & f_1 - l_1 \frac{g_0}{\hat{g}_0 + \lambda} \hat{f}_1 \end{bmatrix}, \tag{11}$$

which is further decomposed into

$$A_c = \begin{bmatrix} 0 & 1 \\ k_1 l_1 \hat{f}_2 & k_2 l_2 \hat{f}_1 \end{bmatrix} + \begin{bmatrix} 0 & 0 \\ f_2 - \hat{f}_2 & f_1 - \hat{f}_1 \end{bmatrix} \triangleq \hat{A}_0 + \delta A, \tag{12}$$

where

$$k_1 = \frac{1}{l_1} - \frac{1}{l_2} \frac{g_0}{\hat{q}_0 + \lambda}, \quad k_1 > 0, \quad k_2 = l_2 + l_1 k_1.$$
 (13)

Note that the simple relationship between  $k_1$  and  $k_2$  is because of the unique property of the golden-section parameters  $l_1$  and  $l_2$  that  $l_1 = l_2^2$ .

**Theorem 1.** Given a time instance k, there exists  $\lambda \in \mathbb{R}$  such that when  $\hat{\Gamma} \in D_s$ ,  $\hat{A}_0$  is stable in the discrete domain.

Proof. See Appendix A.

The system matrices  $\hat{A}_0$  and  $A_c$  are full rank matrices that are diagonalized by  $\hat{\Lambda} = \hat{X}^{-1}\hat{A}_0\hat{X}$  and  $\Lambda = X^{-1}A_cX$ , respectively, where

$$\hat{X} = \begin{bmatrix} 1 & 1 \\ \frac{k_2 l_2 \hat{f}_1 + \sqrt{M}}{2} & \frac{k_2 l_2 \hat{f}_1 - \sqrt{M}}{2} \end{bmatrix} \text{ or } \hat{X} = \begin{bmatrix} 1 & 1 \\ \frac{k_2 l_2 \hat{f}_1 + i\sqrt{M}}{2} & \frac{k_2 l_2 \hat{f}_1 - i\sqrt{M}}{2} \end{bmatrix}$$

is the eigenvector matrix with its inverse

$$\hat{X}^{-1} = \frac{-1}{\sqrt{|M|}} \begin{bmatrix} \frac{k_2 l_2 \hat{f}_1 - \sqrt{M}}{2} & -1 \\ -\frac{k_2 l_2 \hat{f}_1 + \sqrt{M}}{2} & 1 \end{bmatrix} \quad \text{or} \quad \hat{X}^{-1} = \frac{-1}{i\sqrt{|M|}} \begin{bmatrix} \frac{k_2 l_2 \hat{f}_1 - i\sqrt{M}}{2} & -1 \\ -\frac{k_2 l_2 \hat{f}_1 + i\sqrt{M}}{2} & 1 \end{bmatrix}.$$

It has been well-established that the sensitivity of the eigenvalues subject to perturbations is determined by the condition number of the eigenvectors [38]. That is,

$$\|\delta\Lambda\| = \|\hat{\Lambda} - \Lambda\| \leqslant \|\hat{X}^{-1}\| \|\hat{X}\| \|\delta A\| = \kappa(\hat{X}) \|\delta A\|, \tag{14}$$

where  $\kappa(\hat{X})$  is the condition number of  $\hat{X}$ .

**Theorem 2.** Consider the characteristic model (2) whose characteristic parameters are estimated within the convex set  $D_s$ . For a triplet  $\hat{\Gamma}$  and given a time instance k, the closed-loop system  $A_c$  in (12) is stable if there exists  $\lambda$  such that  $\hat{A}_0$  in (12) is stable.

*Proof.* When  $\hat{A}_0$  is stable in the discrete domain,  $|\hat{X}(2,1)| < 1$  and  $|\hat{X}(2,2)| < 1$ . Let  $\|\cdot\|$  be the  $L_2$  norm, then according to the well-known inequality

$$\max_{i,j} |a_{ij}| \leqslant ||A||_2 \leqslant \sqrt{mn} \max_{i,j} |a_{ij}|, \quad A = [a_{ij}] \in \mathbb{R}^{m \times n},$$

the condition number  $\kappa(\hat{X})$  in (14) is bounded by

$$\kappa(\hat{X}) \leqslant \frac{4}{\sqrt{|k_2^2 l_2^2 \hat{f}_1^2 + 4k_2 \hat{f}_2 - 4l_2 \hat{f}_2|}} = 4/\sqrt{|M|}.$$
 (15)

When  $\hat{A}_0$  is perturbed by  $\delta A$ , the corresponding variation on its spectral radius is bounded by (14). According to the upper bound of the condition number shown in (15), it further yields

$$\|\delta\Lambda\| \leqslant \frac{4}{\sqrt{|M|}} \|\delta A\| \leqslant \frac{4}{\sqrt{|M|}} 2 \max_{1,2} |f_i - \hat{f}_i|.$$

To guarantee  $\rho_{A_c} < 1$ , it is equivalent that  $\rho_{A_c} - \rho_{\hat{A}_0} < 1 - \rho_{\hat{A}_0}$ , whose sufficient condition is

$$\frac{4}{\sqrt{|M|}} 2 \max_{1,2} |f_i - \hat{f}_i| < 1 - \rho_{\hat{A}_0},$$

or equivalently,

$$64 \max |f_i - \hat{f}_i|^2 < |M|(1 - \rho_{\hat{A}_0})^2. \tag{16}$$

When  $k_2$  belongs to (A8), (A9), or (A10), |M| is bounded and  $\rho_{\hat{A}_0}$  is also upper bounded by  $\epsilon < 1$ . Recall that the characteristic parameters  $f_i$  and  $\hat{f}_i$  belong to the set  $D_s$ , whose bound is determined by the open-loop characteristics and the sampling time. Thus, as long as the sampling time is small enough so as to restrain the estimation errors within a reasonable bound, there always exists an appropriate  $k_2$  that provides adequate stability margin such that inequality (16) is satisfied. The parameter  $\lambda$ , which is uniquely determined by  $k_1$  or  $k_2$ ,  $g_0$  and  $\hat{g}_0$ , is further calculated to guarantee the asymptotic stability of the closed-loop system under the golden-section adaptive control law (3).

**Remark 3.** Theorem 2 proves the stability of  $A_c$  at each time instance k. The stability of the closed-loop system over the entire time span can be proved based on the stability criterion of slowly time-varying system, as in [39,40].

When the dimension of  $A_c$  increases, Theorem 2 applies consistently, as compared to root locus-based analysis [37] that is restricted to low-order system.

Notice that u(k) in (3) is a time-varying controller whose coefficients are identified online. Thus it is significant to find an efficient way to solve  $\lambda$  online during each time interval as in (8), rather than choosing an identical  $\lambda$  offline.

However, there lacks an analytical method to determine the exact value of  $\lambda(k)$  during controller design. Although Theorems 1 and 2 give the feasible region for  $\lambda(k)$ , it is not suitable for online computing as the design of  $k_2$  and sampling time  $\Delta_t$  is a recursive process. In particular, finding an appropriate  $\Delta_t$  to guarantee condition (16) is blind. At the current stage, it consumes a large amount of time to guess an appropriate  $\lambda(k)$  in practice. Meanwhile, although  $\lambda(k)$  is not unique, at the current stage, picking up  $\lambda$  is a random process as the relationship between  $\lambda$  and the performance of the closed-loop system is unknown. Thus, it is demanding to find an effective and reliable way to compute  $\lambda(k)$  such that the closed-loop system is stable and the  $H_2$  and  $H_{\infty}$  performances are guaranteed. This problem is explored in the next two sections from the state feedback control perspective and the output feedback control perspective, respectively.

## 3.2 State feedback-based parametrization

In the attitude control of hypersonic cruise vehicles, the attitude angles are measurable. Without loss of generality, choose the measured output matrix  $C_2 = [0 \ 1]$ , and the golden-section adaptive control law is then treated as a state feedback control law where the LMI-based criterions are well-developed. In the following context it will be shown that the golden-section control law is a structured state feedback law where challenges arise during the synthesis of  $\lambda(k)$ .

Setting the states  $x_1(k) = y(k-1)$ ,  $x_2(k) = y(k)$ , system (2) under control law (8) is then

$$\begin{bmatrix} x_1(k+1) \\ x_2(k+1) \end{bmatrix} = \tilde{A}_c(k) \begin{bmatrix} x_1(k) \\ x_2(k) \end{bmatrix} + B_1 w(k), \tag{17}$$

and the controlled output is

$$z(k+1) = C_1 \mathbf{x}(k), \tag{18}$$

where

$$\tilde{A}_c(k) = \begin{bmatrix} 0 & 1 \\ f_2(k) - l_2 \frac{g_0(k)}{\hat{g}_0(k) + \lambda(k)} \hat{f}_2(k) & f_1(k) - l_1 \frac{g_0(k)}{\hat{g}_0(k) + \lambda(k)} \hat{f}_1(k) \end{bmatrix},$$

 $B_1 = [0 \ 1]^{\mathrm{T}}$ , and  $C_1 = [0 \ 1]$ . When  $w(k) \in L_2$ , the output z corresponds to the  $H_{\infty}$  performance, and when  $w(k) \in L_{\infty}$ , it corresponds to the  $H_2$  performance.

Matrix  $\tilde{A}_c(k)$  is a time-varying system matrix because of the time varying nature of  $f_i$ ,  $g_i$  and the updates of  $\hat{f}_i$  and  $\hat{g}_i$ . Parameter  $\lambda(k)$  is also calculated at each sampling time simultaneously. In the remaining context, (k) is usually omitted for simplicity.

During each sampling interval,  $\tilde{A}_c$  is decomposed into

$$\tilde{A}_c = \begin{bmatrix} 0 & 1 \\ f_2 & f_1 \end{bmatrix} + \begin{bmatrix} 0 & 0 \\ -l_2 \frac{g_0}{\hat{g}_0 + \lambda} \hat{f}_2 & -l_1 \frac{g_0}{\hat{g}_0 + \lambda} \hat{f}_1 \end{bmatrix} = \begin{bmatrix} 0 & 1 \\ f_2 & f_1 \end{bmatrix} + \begin{bmatrix} 0 \\ g_0 \end{bmatrix} \begin{bmatrix} 1 & \mu \end{bmatrix} m \triangleq A_0 + B_2 U m, \tag{19}$$

where  $m = -l_2 \frac{1}{\hat{g}_0 + \lambda} \hat{f}_2$  and  $\mu = \frac{\hat{f}_1 l_1}{\hat{f}_2 l_2}$ .

Matrix  $A_0$  belongs to a diamond determined by four vertexes  $A_{0i}$ , i = 1, ..., 4, as in Figure 1. The control input matrix  $B_2$  belongs to a convex domain determined by two vertexes  $B_{21}$  and  $B_{22}$ . Thus,  $\tilde{A}_C$  belongs to a convex domain determined by eight extreme matrices

$$\Omega_A(A_{Ci}) := \left\{ A(\epsilon) : A(\epsilon) = \sum_{i=1}^8 \epsilon_i A_{Ci}, \epsilon_i \geqslant 0, \sum_{i=1}^8 \epsilon_i = 1 \right\},\tag{20}$$

where  $A_{Ci} = A_{0i} + B_{2i}Um$ . Those extreme matrices are highly related to the plant and the sampling time  $\Delta_t$ .

**Lemma 3.** The closed-loop system (17) with output (18) is exponentially stable with  $J_{\infty} < \gamma_1$  and  $J_2 < \sqrt{\gamma_2}$  if there exist symmetric matrices H and  $N_i$ , i = 1, ..., 8, and a matrix Q of appropriate dimensions such that

$$\begin{bmatrix} N_{i} & A_{Ci}Q & B_{1} & 0\\ Q^{T}A_{Ci}^{T} & Q + Q^{T} - N_{i} & 0 & Q^{T}C_{1}^{T}\\ B_{1}^{T} & 0 & I & 0\\ 0 & C_{1}Q & 0 & \gamma_{1}I \end{bmatrix} > 0,$$

$$(21)$$

$$\begin{bmatrix} H_i & C_1 Q \\ Q^{\mathrm{T}} C_1^{\mathrm{T}} & Q + Q^{\mathrm{T}} - N_i \end{bmatrix} > 0, \tag{22}$$

$$Tr(H_i) < \gamma_2, \tag{23}$$

where  $A_{Ci}$ , i = 1, ..., 8 are the eight extreme matrices in  $\Omega_A$ .

This sufficient condition integrates the  $H_2$  and  $H_{\infty}$  performances, as compared to its origin in [41] where the sufficient conditions for  $H_2$  performance and  $H_{\infty}$  performance are provided in a respective way.

**Remark 4.** Lemma 3 is only a sufficient condition. Thus, if there is no solution to inequalities (21)–(23), it is not contradictory to the existence of  $\lambda$  concluded in [26].

Recalling (19), the extreme matrix  $A_{Ci}$  is an affine function on m. Thus, inequality (21) is a bilinear matrix inequality. A similar problem emerges in our previous work [40] where the bilinear matrix inequality on the scalar m is transformed into a linear matrix inequality form by introducing a certain degree of conservativeness. In this paper, to find a feasible way to determine m rather than solving the NP-hard BMI problem in Lemma 3, the following theory provides an effective way.

**Theorem 3.** The closed-loop system consisting of (17) and (18) is exponentially stable with  $J_{\infty} < \gamma_1$  and  $J_2 < \sqrt{\gamma_2}$ , if there exist symmetric matrices H and  $N_i$ , i = 1, ..., 8, and a matrix Q such that Eqs. (24a) (or (24b)), (25), and (26) are satisfied.

 $\min \ \tau + \gamma_2$ 

s.t.

$$\Sigma_{i} < \tau \begin{bmatrix} N_{i} & (A_{0i} + B_{2i}U)Q B_{1} & 0\\ Q^{T}(A_{0i} + B_{2i}U)^{T} & Q + Q^{T} - N_{i} & 0 & Q^{T}C_{1}^{T}\\ B_{1}^{T} & 0 & I & 0\\ 0 & C_{1}Q & 0 & \gamma_{1}I \end{bmatrix}, m < 1, \tau = \frac{1}{1 - m},$$
 (24a)

$$-\Sigma_{i} < \tau \begin{bmatrix} N_{i} & (A_{0i} + B_{2i}U)Q B_{1} & 0\\ Q^{T}(A_{0i} + B_{2i}U)^{T} & Q + Q^{T} - N_{i} & 0 & Q^{T}C_{1}^{T}\\ B_{1}^{T} & 0 & I & 0\\ 0 & C_{1}Q & 0 & \gamma_{1}I \end{bmatrix}, m > 1, \tau = \frac{1}{m-1},$$
 (24b)

$$\begin{bmatrix} H_i & C_1 Q \\ Q^{\mathrm{T}} C_1^{\mathrm{T}} & Q + Q^{\mathrm{T}} - N_i \end{bmatrix} > 0,$$
 (25)

$$Tr(H_i) < \gamma_2, \ \forall i = 1, \dots, 8, \tag{26}$$

where

*Proof.* Substituting  $\tilde{A}_{Ci}$  into (21) yields

$$\begin{bmatrix} N_{i} & (A_{0i} + B_{2i}U)Q B_{1} & 0 \\ Q^{T}(A_{0i} + B_{2i}U)^{T} & Q + Q^{T} - N_{i} & 0 & Q^{T}C_{1}^{T} \\ B_{1}^{T} & 0 & I & 0 \\ 0 & C_{1}Q & 0 & \gamma_{1}I \end{bmatrix} > (1 - m)\Sigma_{i}.$$

$$(27)$$

Condition (21) in Lemma 3 is equivalent to inequality (27), which, when m < 1, is equivalent to (24a), and when m > 1, is equivalent to (24b). Conditions (24a) (or (24b)), (25), and (26) is then a generalized eigenvalue problem.

When m < 1,

$$\Sigma_{i} < \tau \left( \begin{bmatrix} N_{i} & (A_{0i} + B_{2i}U)Q \ B_{1} \\ Q^{T}(A_{0i} + B_{2i}U)^{T} & Q + Q^{T} - N_{i} & 0 \\ B_{1}^{T} & 0 & I \end{bmatrix} - \frac{1}{\gamma_{1}}Q^{T}C_{1}^{T}C_{1}Q \right).$$

Recalling that  $C_1 = [0 \ 1]$ , it is easy to conclude that  $Q^T C_1^T C_1 Q$  is positive semidefinite. Thus, m is proportional to  $\gamma$ . By minimizing  $\tau = \frac{1}{1-m}$ , the minimum of m corresponds to the minimum of  $\gamma_1$ . When m > 1, the maximum of m corresponds to the minimum of  $\gamma_1$ . Thus, the generalized eigenvalue problem results in the optimal  $\gamma_1 + \gamma_2$ , which corresponds to the optimal  $H_2$  and  $H_{\infty}$  performances.

By introducing weighting coefficients to  $\tau$  and  $\gamma_2$ , more flexible design objectives could be covered so as to suit different control requirements.

**Remark 5.** This generalized eigenvalue optimization problem can be solved using "gevp" in LMI-toolbox.

**Remark 6.** The situation when m = 1 is not included in the theorem. According to (27), when m = 1, it is a positive definite problem.

Based on Lemma 3, Theorem 3 further provides a feasible way to determine m such that the  $H_2$  and  $H_{\infty}$  performances are optimized. In other words, the dynamic performance of the system with w(k) is optimized when  $\lambda(k)$  is parameterized according to Theorem 3.

#### 3.3 Static output feedback-based parametrization

In this section, parameter  $\lambda(k)$  is further explored under the static output feedback control scheme. Although the golden-section adaptive control law is an output feedback control law, the feedback gain is a  $1 \times 2$  matrix with a particular structure, that is, the two entries are a convex combination of two extreme values determined by the characteristic model of the plant. According to the analysis in the previous section, when determining the parameter  $\lambda(k)$  or m in (19), the structural restriction on the feedback control gain is not guaranteed by the conventional feedback controller synthesis. Compared to the state feedback-based parametrization method, in this section the design of parameter  $\lambda(k)$  is investigated through the output feedback perspective.

To ensure that the control input preserves the specific structure of the golden-section adaptive control law, the output matrix in the state-space equation of the characteristic model-based system (17) is rewritten into the following form

$$\begin{bmatrix}
x_1(k+1) \\
x_2(k+1)
\end{bmatrix} = A_0(k) \begin{bmatrix} x_1(k) \\
x_2(k) \end{bmatrix} + B_1 w(k) + B_2(k) u(k),$$

$$z(k) = C_1 \begin{bmatrix} x_1(k) \\ x_2(k) \end{bmatrix} + D_{11} w(k) + D_{12} u(k),$$

$$\tilde{y}(k) = C_2(k) \begin{bmatrix} x_1(k) \\ x_2(k) \end{bmatrix},$$
(28)

where

$$A_0(k) = \begin{bmatrix} 0 & 1 \\ f_2(k) & f_1(k) \end{bmatrix}, \quad B_1 = \begin{bmatrix} 0 \\ 1 \end{bmatrix}, \quad B_2(k) = \begin{bmatrix} 0 \\ g_0(k) \end{bmatrix}, \quad C_1 = \begin{bmatrix} 0 & 1 \end{bmatrix}, \quad C_2(k) = -\begin{bmatrix} l_2 \hat{f}_2(k) & l_1 \hat{f}_1(k) \end{bmatrix}.$$

It is assumed that the measured output  $\tilde{y}(k)$  is not corrupted by the disturbance w(k).

The closed-loop system under output feedback controller

$$u(k) = K(k)\tilde{y}(k), \quad K(k) \in \mathbb{R}$$
 (29)

is then

$$\mathbf{x}(k+1) = (A_0(k) + B_2(k)K(k)C_2(k))\mathbf{x}(k) + B_1w(k),$$
  

$$\mathbf{z}(k) = (C_1 + D_{12}K(k)C_2(k))\mathbf{x}(k) + D_{11}w(k),$$
(30)

where  $x = [y(k-1) \ y(k)]^{T}$ .

Thus, the system matrix  $A_0$  in (28) is such that  $A_0 \in \Omega_{A_0}(A_{0i})$ , where N in (20) equals four, and  $B_2 \in \Omega_B(B_{2i})$ , where N = 2.

The controlled output matrix  $C_2 \in \Omega_C(C_{2i})$ , where N=4 and  $C_{2i}=-[l_2\bar{f}_{2i} \ l_1\bar{f}_{1i}]$  is of full rank whose UR decomposition is

$$C_{2i} = UR_i = \begin{bmatrix} 1 & 0 \end{bmatrix} \begin{bmatrix} -l_2 \bar{f}_{2i} & -l_1 \bar{f}_{1i} \\ 0 & 1 \end{bmatrix}.$$

**Theorem 4.** The closed-loop system (28) is exponentially stable with  $J_{\infty} < \gamma_1$  and  $J_2 < \sqrt{\gamma_2}$ , if there exist symmetric matrices  $Q_i$ ,  $1 \le i \le 4$  and matrices  $M_{ij} \in \mathbb{R}^{2 \times 2}$ ,  $P \in \mathbb{R}^{1 \times 2}$  with

$$M_{ij} = \begin{bmatrix} m_1 & 0 \\ m_{21}^{ij} & m_{22}^{ij} \end{bmatrix}, \quad P = \begin{bmatrix} p_1 & 0 \end{bmatrix},$$

such that

$$\begin{bmatrix} Q_{i} - R_{i}m_{ij} - m_{ij}^{\mathrm{T}}R_{i}^{\mathrm{T}} & * & * & * \\ A_{0i}R_{i}m_{ij} + B_{2j}P & -Q_{l} & * & * & * \\ C_{1}R_{i}m_{ij} + D_{12}P & 0 & -\epsilon I & * \\ 0 & B_{1}^{\mathrm{T}} D_{11}^{\mathrm{T}} - \gamma_{1}I \end{bmatrix} < 0, \quad i, l = 1, \dots, 4, \quad j = 1, 2,$$

$$(31)$$

$$\begin{bmatrix} -Z_i & * \\ B_1 & -Q_i \end{bmatrix} < 0, \quad i = 1, 2, 3, 4, \tag{32}$$

$$Tr(Z_i) < \gamma_2, \quad i = 1, 2, 3, 4,$$

where

$$\epsilon = \begin{cases} 1, & \gamma_1 > 1\\ \gamma_1, & \gamma_1 \leqslant 1. \end{cases} \tag{33}$$

The feedback gain  $K = p_1 m_1^{-1}$ .

*Proof.* According to [42], the sufficient condition for asymptotic stability of the closed-loop system under  $K = p_1 m_1^{-1}$  is

$$\begin{bmatrix} -N_i & * \\ N_i(A_{0i}R_im_{ij} + B_{2j}P) & -N_l \end{bmatrix} < 0, \quad i, l = 1, \dots, 4, \quad j = 1, 2,$$

where  $N_i = Q_i^{-1}$ . It then yields

$$\sum_{j=1}^{2} \sum_{l=1}^{4} \sum_{i=1}^{4} \alpha_{j} \alpha_{l} \alpha_{i} \begin{bmatrix} -N_{i} & * \\ N_{i} (A_{0i} R_{i} m_{ij} + B_{2j} P) & -N_{l} \end{bmatrix} < 0, \quad i, l = 1, \dots, 4, \quad j = 1, 2.$$

Recalling that  $\sum_{j=1}^{2} \alpha_{j} = 1$ ,  $\sum_{l=1}^{4} \alpha_{l} = 1$ , and  $\sum_{i=1}^{4} \alpha_{i} = 1$ , according to Schur Complement and by choosing the Lyapunov function  $V(k) = x^{T}(k)(\sum_{i=1}^{4} \alpha_{i}(k)N_{i})x(k)$ , the conclusion of asymptotic stability is obtained.

Also, the sufficient condition for  $H_{\infty}$  performance of the closed-loop system under the output feedback controller  $K = p_1 m_1^{-1}$  is

$$\begin{bmatrix} Q_{i} - R_{i}m_{ij} - m_{ij}^{\mathrm{T}}R_{i}^{\mathrm{T}} & * & * & * \\ 0 & -\gamma_{1}I & * & * \\ A_{0i}R_{i}m_{ij} + B_{2j}P & B_{1i} & -Q_{l} & * \\ C_{1i}R_{i}m_{ij} + D_{12i}P & 0 & 0 & -\epsilon I \end{bmatrix} < 0, \quad i, l = 1, \dots, 4, \quad j = 1, 2,$$

$$(34)$$

which further yields inequality (31).

The  $H_2$  performance is bounded by (32) with the upper bound of  $\gamma_2$  being guaranteed by (33), which finishes the proof.

## **Remark 7.** The UR decomposition is unique. Thus, $R_i$ is uniquely determined by $C_{2i}$ .

Static output feedback controller design with polytopic uncertainties has been well-developed over the past years. By modifying the output matrix, we attribute the golden-section adaptive control law to the framework of static output feedback control such that the existing results are available to be inherited.

The static output feedback-based parametrization method provides a less conservative way to determine the parameter  $\lambda(k)$ , as compared with the state feedback-based method.

# 4 Attitude control of hypersonic cruise vehicles

Simulations are carried out on a hypersonic cruise vehicle weighting 4353 kg with length 12.7 m. The moment of inertia for the pitching movement is  $J_y = 34979 \text{ kgm}^2$ , the one for the yaw movement is  $J_z = 39924 \text{ kgm}^2$ , and the one for the roll movement is  $J_x = 723 \text{ kgm}^2$ . The input to the longitudinal plane is the elevon control surface deflection  $\delta_e$ , and the inputs to the lateral-directional plane are aileron deflections and rudder deflections, respectively.

For a robust adaptive control scheme, in the large time scale, the system depends on the adaption of the parameters  $\hat{f}_i$ ,  $\hat{g}_0$  in (8) to restrain the states stay close to the commanded value, and during each sampling interval, we relay on  $\lambda(k)$  in particular for the robust transient performance. Note that the characteristic model during the re-entry phase of hypersonic vehicle is time-varying. Thus the estimation error is consistently nonzero. This control scheme integrates adaptive control and robust control in a cooperative way. In the previous section, stability of the closed-loop system at each time instance k has been proved. The stability of the closed-loop slowly time-varying system over the entire time span was proved in our previous work [40].

#### 4.1 Attitude control during the gliding phase: state feedback-based parameterizations

During the gliding phase between an altitude of about 35–60 km, the vehicle maneuvers in a small scale and the flying environment is relatively benign, compared to the vehicle in the TAEM phase or the pull-up phase. In our previous work, both golden-section adaptive control law and golden-section time-invariant control law have been applied to the attitude control during the gliding phase [43]. According to the simulation results, time-invariant golden-section control law provides comparatively satisfying tracking performance in compared to system under the golden-section adaptive control law. Thus, in this section, the extreme matrixes of the prism is set to be constant during the gliding phase, and the parameter  $\lambda$  in the golden-section control law is fixed and is calculated offline.

The gliding phase is initialized at an altitude of 42 km and a velocity of 2.5 km/s. The commanded angle of attack (AOA) and roll angle varies between 0 and 6 degrees. The sideslip angle is expected to stay at zero. Disturbances consist of windage and absolute uncertainties on the angle of attack appear at t = (8k+3) s,  $k = 0, 1, \ldots$ , each of which lasts for 0.8 s with an amplitude of 2 degrees. The disturbances to the roll angle appear at t = (5k+3) s,  $k = 1, 2, \ldots$  with an amplitude of 3 degrees and width 0.25 s. According to Theorem 3, the optimal controller parameters for the angle of attack, roll angle and the sideslip angle, as denoted by  $m_{\alpha}^*$ ,  $m_{\theta}^*$ ,  $m_{\beta}^*$ , are calculated using the "gevp" command in the LMI-toolbox. To show the optimality, two additional sets of  $\{m_{\alpha}, m_{\theta}, m_{\beta}\}$  are randomly chosen for comparison purpose, and the simulation results are recorded in Table 1 as well. The tracking of the three angles under the optimal  $\{m_{\alpha}^*, m_{\theta}^*, m_{\beta}^*\}$  are shown in Figure 2(a). Comparisons on the tracking performance of the angle of attack, roll angle, and the sideslip angle among different controller parameters are shown in Figure 2 (b)–(d), respectively.

The attitude system is stable under all three cases in Table 1. According to the table, the  $H_2$  and  $H_{\infty}$  norm of the tracking errors under the set  $\{m_{\alpha}^*, m_{\theta}^*, m_{\beta}^*\} = \{400, 50, 430\}$  is the smallest among the

		$m_{lpha}$	$m_{ heta}$	$m_eta$	$H_2$			$H_{\infty}$		
					$\alpha$	θ	β	$\alpha$	θ	β
Set 1	1*	400	50	430	2.0399	3.5847	0.2610	26.2686	36.8598	2.9003
	2	120	19	130	2.4154	4.1677	0.5166	31.1797	41.1991	5.0501
	3	639	300	606	2.0640	3.6327	0.2610	41.5950	50.1657	3.1980
Set 2	1*	500	100	430	2.0428	3.3065	0.2700	25.5526	36.5474	3.0026
	2	120	19	130	2.4211	4.1835	0.4909	31.1910	43.9708	5.5247
	3	639	300	606	2.0637	3.5018	0.2700	42.6507	49.6544	4.0889
Set 3	1*	480	120	430	2.0409	3.2512	0.4728	26.0056	39.4361	5.0624
	2	120	19	130	2.4211	4.1835	0.6520	31.1233	48.3117	7.0478
	3	639	300	606	2.0657	3.4836	0.4728	45.7326	50.3341	8.5016

Table 1  $H_2$  and  $H_\infty$  performances under different m: state feedback-based

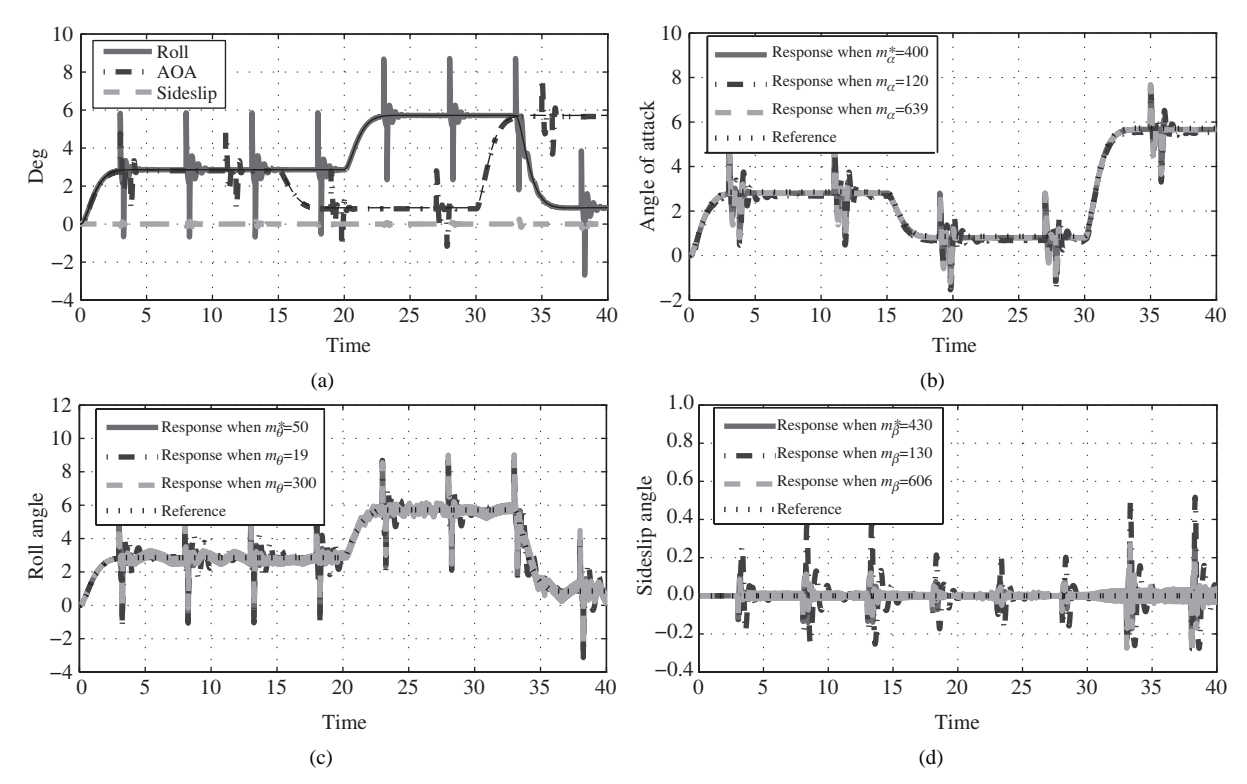


Figure 2 Simulations under commanded angle set 1: state feedback-based. (a) Tracking of the three angles under  $\{m_{\alpha}^*, m_{\theta}^*, m_{\beta}^*\}$ ; (b) tracking of the angle of attack under different  $m_{\alpha}$ ; (c) tracking of the roll angle under different  $m_{\theta}$ ; (d) tracking of the sideslip angle under different  $m_{\beta}$ .

three cases. In case 2, the parameters are smaller than the optimal set and in case 3, the parameters are larger than the optimal set, both of which result in higher  $H_2$  and  $H_\infty$  gains, indicating that the attitude system is more sensitive to external disturbances and aerodynamic coefficients uncertainties compared to that of case 1. In other words, although in the presence of windage and uncertainties, the attitude system under the golden-section adaptive control law with parameters given in Table 1 is stable in all the three cases, the attitude system under parameter set  $\{m_\alpha^*, m_\theta^*, m_\beta^*\}$  has the best dynamic performance among the three cases, and thus can tolerate the largest scale of absolute coefficient errors. The effectiveness of the proposed state feedback-based parametrization method is verified.

Figures 3 and 4 show another two similar simulations when tracking different angle sets. The  $H_2$  performance and  $H_{\infty}$  performance are shown in Table 1 as well. The numerical results also verify the proposed method.

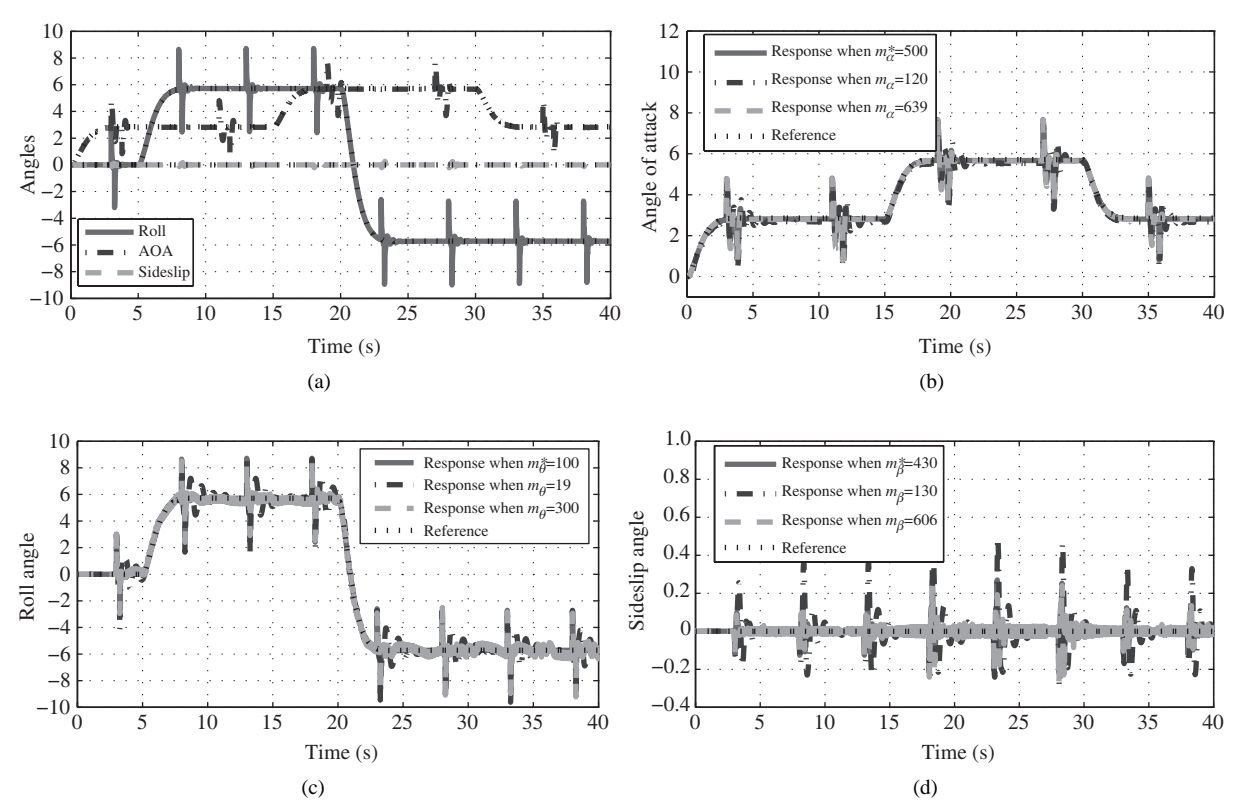


Figure 3 Simulations under commanded angle set 2: state feedback-based. (a) Tracking of the three angles under  $\{m_{\alpha}^*, m_{\theta}^*, m_{\theta}^*\}$ ; (b) tracking of the angle of attack under different  $m_{\alpha}$ ; (c) tracking of the roll angle under different  $m_{\theta}$ ; (d) tracking of the sideslip angle under different  $m_{\theta}$ .

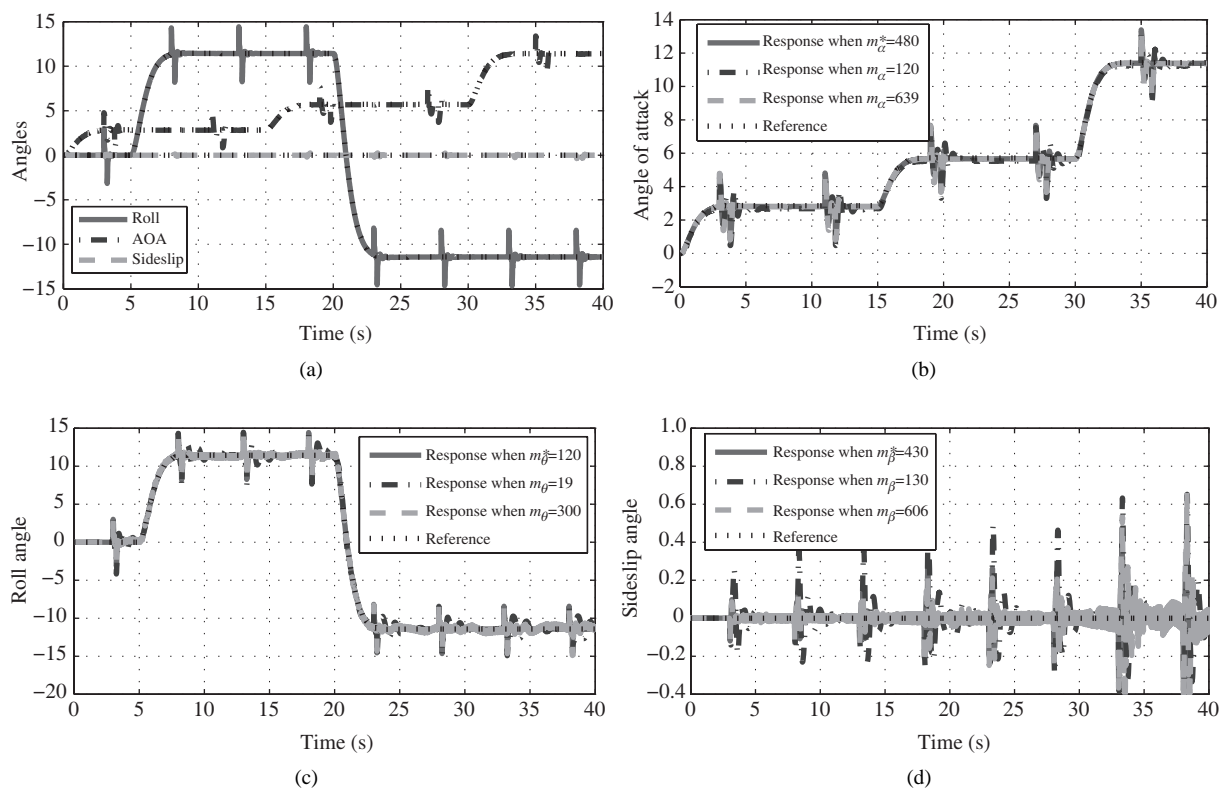


Figure 4 Simulations under commanded angle set 3: state feedback-based. (a) Tracking of the three angles under  $\{m_{\alpha}^*, m_{\theta}^*, m_{\beta}^*\}$ ; (b) tracking of AOA under different  $m_{\alpha}$ ; (c) tracking of the roll angle under different  $m_{\theta}$ ; (d) tracking of the sideslip angle under different  $m_{\beta}$ .

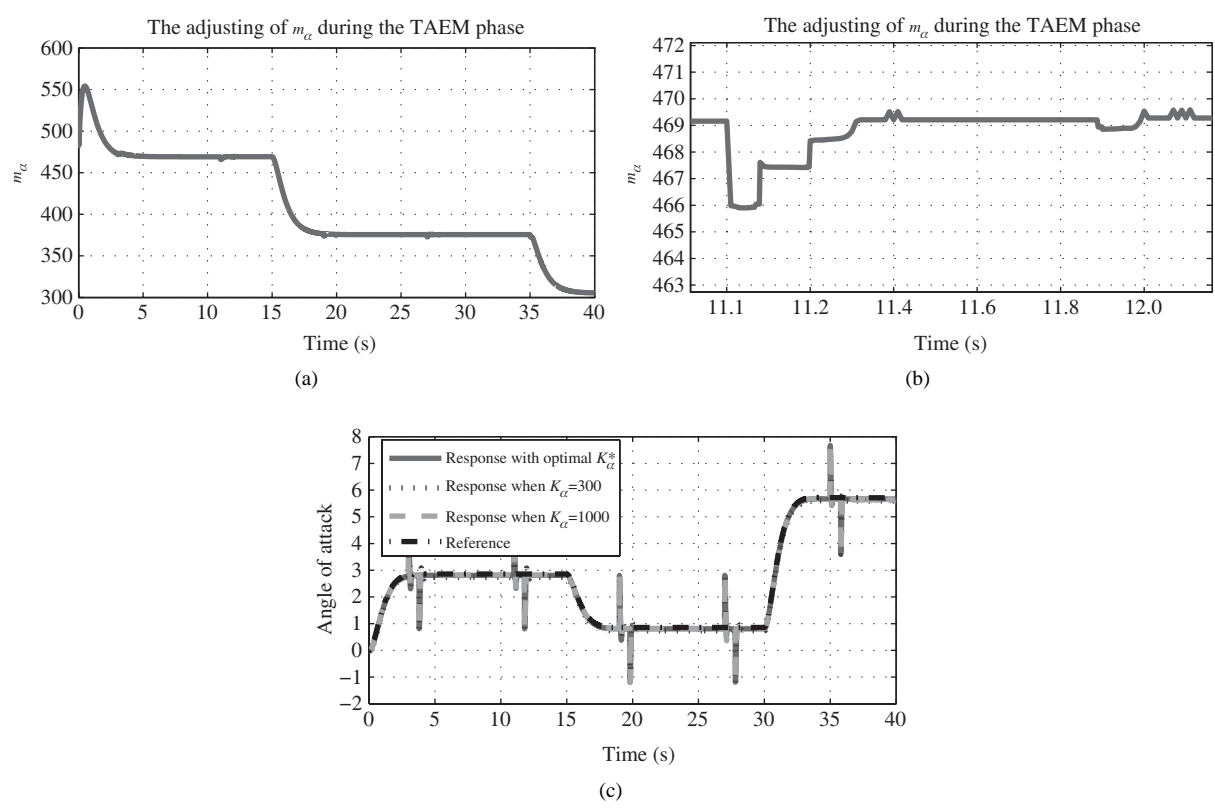


Figure 5 TAEM Simulations under commanded AOA 1. Windage and absolute uncertainties appear at t=3 s, 11 s, 19 s, . . . . (a) Online adjusting of  $m_{\alpha}(k)=-l_2\hat{f}_2K_{\alpha}(k)$  under the output feedback-based parametrization; (b) zoomed in; (c) tracking of the AOA under different  $K_{\alpha}$ .

## 4.2 Attitude control during the TAEM phase: output feedback-based parameterizations

To further demonstrate the advantages of the golden-section robust adaptive control law that is designed to accommodate large range of flight conditions, the TAEM phase initialized at an altitude of 33 km and a velocity of 2.0 km/s is considered. Disturbance w acting on the AOA is simulated by a periodic pulse signal at time t = (8k+3) s,  $k = 0, 1, \ldots$  with an amplitude of 3 degrees and width 0.25 s. For the TAEM phase, because of the fact that the lateral-directional dynamics are strongly coupled such that the SISO characteristic model dose not fit, we only focus on the longitudinal dynamics, that is, the control of AOA. According to Theorem 4, a series of the output feedback control gain  $K_{\alpha}(k)$  in (30) is calculated online at different sets of parameter bounds. For easy comparison to the state feedback-based parametrization, the value of  $K_{\alpha}(k)$  in (29) is transmitted to m in (19), as shown in Figure 5(a). The transient performance when tracking the commanded AOA is shown in Figure 5(c) under the optimal control gain  $K_{\alpha}^{*}(k)$ , as compared to the transient performance under some randomly chosen and constant parameters  $K_{\alpha} = 300$  and  $K_{\alpha} = 1000$ . The  $H_{2}$  norm and  $H_{\infty}$  norm of the tracking errors in the presence of disturbance are recorded in Table 2.

According to Figure 5(a), compared to  $m^*(\alpha)$  during the gliding phase in Table 1,  $K_{\alpha}^*(k)$  is adjusted near  $m^*(\alpha)$ , which indicates that the characteristic parameters bounds are relatively stable during reentry. However, when the angle of attack experiences a sudden change because of disturbances, for example, at t=11 s,  $K_{\alpha}(k)$  also shows a sudden decrease so as to restrict the  $H_2$  and  $H_{\infty}$  gain within a satisfying level, as in Figure 5(b). The value of  $K_{\alpha}(k)$  tends to decrease, indicating that the estimation of  $\hat{g}_0$  tends to increase as the vehicle descends during the TAEM phase. This observation coincide with the practical experience that when the velocity decelerate is relatively slow as compared to the increase of the atmospheric density such that the dynamic pressure increases, it produces stronger control efforts at the same elevon deflection.

Smaller tracking errors and more stronger robustness to external disturbances and aerodynamic coef-

		$K_{\alpha}$	$H_2$	$H_{\infty}$
	1*	$\{K_{\alpha}(k)\}$	2.0493	19.9486
AOA 1	2	300	2.1262	21.5565
	3	1000	2.0718	22.5941
	1*	$\{K_{\alpha}(k)\}$	2.0321	20.3343
AOA 2	2	200	2.1261	21.4657
	3	800	2.0364	23.1529

**Table 2**  $H_2$  and  $H_\infty$  performances of AOA under different  $K_\alpha$ : output feedback-based

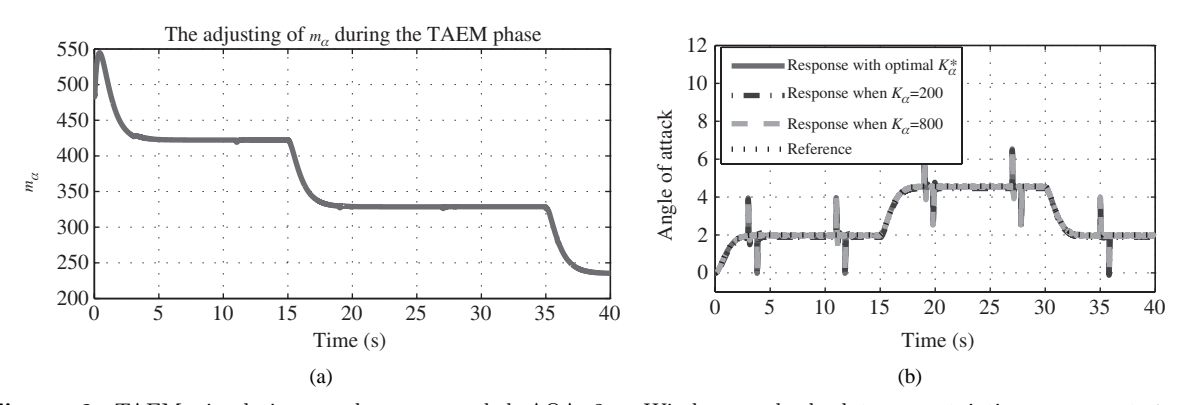


**Figure 6** TAEM simulations under commanded AOA 2. Windage and absolute uncertainties appear at  $t = 3 \text{ s}, 11 \text{ s}, 19 \text{ s}, \dots$  (a) overall  $m_{\alpha}$  during the TAEM phase; (b) tracking of the AOA under different  $K_{\alpha}$ : output feedback-based.

ficients uncertainties are observed under the optimal control gain in Table 2, which validates the effectiveness of the output feedback-based parameterizing algorithm.

Figure 6 and Table 2 show another similar simulation when tracking a different angle of attack. The numerical results also verify the proposed method.

## 5 Conclusion

This paper focused on robust adaptive control of a lifting body hypersonic cruise vehicle. The characteristic model with prominent practical privileges is introduced to the attitude dynamics of hypersonic cruise vehicles. When designing the golden-section adaptive control law, linear matrix inequality-based criterions are proposed to determine the parameter  $\lambda$  in the control law such that the  $H_2$  and  $H_{\infty}$  performances are guaranteed. In the robust adaptive control scheme, the large flight conditions are accommodated by the adaption of the characteristic parameters, and the external disturbance and absolute errors on the aerodynamic coefficients are compensated by the online adjusting of  $\lambda(k)$ . Experimental results verified the effectiveness of the proposed method.

Future work would be in the extension of the results to multiple-input-multiple-output characteristic model which incorporates the coupling between the longitudinal dynamics and the lateral-directional dynamics. In such a case, several  $\lambda(k)$  at different angles should be adjusted simultaneously, which increases the dimension of the problem.

#### Acknowledgements

This work was supported by National Natural Science Foundation of China (Grant Nos. 61203075, 61333008). The authors would like to thank Professor Wu H X for the insightful comments and discussions, which have significantly improved the presentation of this work. Thanks are also due to anonymous reviewers for their valuable comments.

#### References

- 1 Peebles C. The X-43A Flight Research Program Lessons Learned on the Road to Mach 10. Technical Report, Dryden Flight Research Center, 2007
- 2 Fidan B, Mirmirani M, Ioannou P A. Flight dynamics and control of air-breathing hypersonic vehicles: review and new directions. In: Proceedings of ther 12th AIAA International Space planes and Hypersonic Systmes and Technologies, Norfolk, 2003
- 3 Huang L, Duan Z S, Yang J Y. Challenges of control science in near space hypersonic aircrafts (in Chinese). Contr Theor Appl, 2011, 28: 1496–1505
- 4 Lind R. Linear parameter-varying modeling and control of structural dynamics with aerothermoelastic effects. J Guid Contr Dynam, 2002, 25: 733–739
- 5 Somanath A, Annaswamy A. Adaptive control of hypersoinc vehicles in presence of aerodynamic and certer of gravity uncertainties. In: Proceedings of the 49th IEEE Conference on Decision and Control, Atlanta, 2010. 4661–4666
- 6 Fiorentini L, Serrani A, Bolender M A, et al. Nonlinear robust adaptive controller design for an air-breathing hypersonic vehicle model. In: Proceedings of the 2007 AIAA Guidance, Navigation and Control Conference and Exhibit, South Carolina, 2007
- 7 Gregory I M, McMinn J D, Shaughnessy J D, et al. Hypersonic Vehicle Control Law Development Using  $H_{\infty}$  and  $\mu$  Synthesis. Technical Report, Langley Research Center N94-25104, 1993
- 8 Xu H J, Mirmirani M D, Ioannou P A. Adaptive sliding mode control design for a hypersonic flight vehicle. J Guid Contr Dynam, 2004, 27: 829–838
- 9 Brinker J S, Wise K A. Flight testing of reconfigurable control law on the X-36 tailless aircraft. J Guid Contr Dynam, 2001, 24: 903–909
- 10 Johnson E N, Calise A J. Limited authority adaptive flight control for reusable launch vehicles. J Guid Contr Dynam, 2003, 26: 906–913
- 11 Gao D X, Sun Z Q. Fuzzy tracking control design for hypersonic vehicles via T-S model. Sci China Inf Sci, 2011, 54: 521–528
- 12 Hughes H, Wu F.  $H_{\infty}$  LPV state feedback control for flexible hypersonic vehicle longitudinal dynamics. In: Proceedings of the 2010 AIAA Guidance, Navigation, and Control Conference, Toronto, 2010
- 13 Cai G B, Duan G R, Hu C H, et al. Tracking control for air-breathing hypersoinc cruise vehicle based on tangent linearization approach. J Syst Eng Electron, 2010, 21: 469–475
- 14 Cheng L, Jiang C S, Pu M. Online-SVR-compensated nonlinear generalized predictive control for hypersonic vehicles. Sci China Inf Sci, 2011, 54: 551–562
- 15 Reiman S E, Dillon C H, Lee H P, et al. Adaptive reconfigurable dynamic inversion control for a hypersonic cruise vehicle. In: Proceedings of AIAA Guidance, Navigation and Control Conference and Exhibit, Honolulu, 2008
- 16 Gibson T E, Crespo L G, Annaswamy A M. Adaptive control of hypersonic vehicles in the presence of modeling uncertainties. In: Proceedings of the 2009 American Control Conference, St. Louis, 2009. 3178–3183
- 17 Wu H X, Hu J, Xie Y C. Characteristic model-based all-coefficient adaptive control method and its applications. IEEE Trans Syst Man Cybern-Part C, 2007, 37: 213–221
- 18 Meng B, Wu H X. A unified proof of the characteristic model of linear time-invariant systems. In: Proceedings of the 2007 American Control Conference, New York, 2007. 935–940
- 19 Li H, Sun Z Q, Min H B, et al. Fuzzy dynamic characteristic modeling and adaptive control of nonlinear systems and its application to hypersonic vehicles. Sci China Inf Sci, 2011, 54: 460–468
- 20 Luo X, Li J. Fuzzy dynamic characteristic model based attitude control of hypersonic vehicle in gliding phase. Sci China Inf Sci, 2011, 54: 448–459
- 21 Wu J G. The study and application of predictive functional control based on characteristic model (in Chinese). Dissertation for the Doctoral Degree. Shanghai: Shanghai University, 2008
- 22 Hu J, Xie Y C, Zhang H, et al. Shenzhou-8 spacecraft guidance navigation and control system and flight result evaluation for rendezvous and docking (in Chinese). Aerosp Contr Appl, 2011, 37: 1–5
- 23 Ma J G, Zhang T, Song J Y. Intelligent attitude control of space target based on characteristic model. In: Proceedings of the 2007 IEEE International Conference on Robotics and Biomimetics, Sanya, 2007. 455–460
- 24 Meng B, Wu H X. Adaptive control based on characteristic model for a hypersonic flight vehicle. In: Proceedings of the 26th Chinese Control Conference, Zhangjiajie, 2007. 720–724
- 25 Meng B, Wu H X, Lin Z L. Characteristic model based control of the X-34 reusable launch vehicle in its climbing phase. Sci China Ser-F: Inf Sci, 2009, 52: 2216–2225
- 26 Meng B, Wu H X. Convergence and stability of the golden-section control (in Chinese). J Astronaut, 2009, 30: 2128–2132
- 27 Wu H X, Hu J, Xie Y C. Characteristic Model-Based Intelligent Adaptive Control (in Chinese). Beijing: China Science and Technology Press, 2009

- 28 Qi C Z, Wu H X, Lv Z D. The study on the stability of all-coefficient golden section feedback control system. In: Proceedings of the 3rd World Congress on Intelligent Control and Automation, Hefei, 2000. 3168–3171
- 29 Bolender M A, Doman D B. A nonlinear longitudinal dynamical model of an air-breathing hypersonic vehicle. J Spacecraft Rocket, 2007, 44: 374–387
- 30 Bollino K P. High-Fidelity Real-Time Trajectory Optimization for Reusable Launch Vehicles. Dissertation for the Doctoral Degree, California: Naval Postgraduate School, 2006
- 31 Souza C E, Xie L H, Coutinho D F. Robust filtering for 2-D discrete-time linear systems with convex-bounded parameter uncertainty. Automatica, 2010, 46: 673–681
- 32 Muradore R, Picci G. Mixed  $H_2/H_{\infty}$  control: the discrete-time case. In: Proceedings of the 42nd IEEE Conference on Decision and Control, Maui, 2003. 1789–1794
- Hwang C L, Han S Y. Mixed  $H_2/H_{\infty}$  design for a decentralized discrete variable structure control with application to mobile robots. IEEE Trans Syst Man Cybern-Part B, 2005, 35: 736–750
- 34 Caigny J D, Camino J F, Oliveira R C L F, et al. Gain-scheduled  $H_2$  and  $H_{\infty}$  control of discrete-time polytopic time-varying systems. IET Contr Theor Appl, 2009, 4: 362–380
- Naidu D S, Banda S S, Buffington J L. Unified approach to  $H_2$  and  $H_{\infty}$  optimal control of a hypersonic vehicle. In: Proceedings of the 1999 American Control Conference, San Diego, 1999. 2737–2741
- 36 Cifdaloz O, Rodriguez A A, Anderies J M. Control of distributed parameter systems subject to convex constraints: applications to irrigation systems and hypersonic vehicles. In: Proceedings of the 47th IEEE Conference on Decision and Control, Cancun, 2008. 865–870
- 37 Yong W. Analysis for several stability properties of all-coefficient adaptive controller (in Chinese). Aerosp Contr Appl, 2012, 38: 10–16
- 38 Li R C. Handook of Linear Algebra. Boca Raton: Chapman and Hall/CRC, 2006. 15-1-15-6
- 39 Guo L. Time-Varying Stochastic Systems (in Chinese). Jilin: Jilin Science and Technology Press, 1993
- 40 Huang H, Wang Y. Mixed H<sub>2</sub>/H<sub>∞</sub> robust adaptive control of hypersonic vehicles based on the characteristic model. In: Proceedings of the 31st Chinese Control Conference, Hefei, 2012. 2883–2888
- 41 Oliveira M C D, Geromel J C, Bernussou J. Extended  $H_2$  and  $H_{\infty}$  norm characterizations and controller parameterizations for discrete-time systems. Int J Contr. 2002, 75: 666–679
- 42 Dong J X, Yang G H. Robust static output feedback control for linear discrete-time systems with time-varying uncertainties. Syst Contr Lett, 2008, 57: 123–131
- 43 Zhang Z. On the guidance and control of hypersonic vehicle with high lift-to-drag ratio (in Chinese). Dissertation of the Doctoral Degree. Beijing: Beijing Institute of Control Engineering, 2011

#### Appendix A Proof of Theorem 1

Let  $\rho_{\hat{A}_0}$  be the spectral radius of  $\hat{A}_0$ . The characteristic polynomial of matrix  $\hat{A}_0$  is determined by M:  $M = k_2^2 l_2^2 \hat{f}_1^2 + 4k_1 l_1 \hat{f}_2$ . Substituting  $k_1$  with  $k_2$  in (13) yields

$$M = k_2^2 l_2^2 \hat{f}_1^2 + 4k_2 \hat{f}_2 - 4l_2 \hat{f}_2.$$

Case 1: the estimations of  $\hat{f}_1$  and  $\hat{f}_2$  are such that  $\hat{f}_2 + l_2^3 \hat{f}_1^2 < 0$ .

In this situation, M has a pair of real eigenvalues as shown in Figure A1. The sufficient condition for M < 0 is

$$\underline{\lambda} < k_2 < \overline{\lambda},\tag{A1}$$

where 
$$\underline{\lambda} = 2 \frac{-\hat{f}_2 - \sqrt{\hat{f}_2^2 + l_2^3 \hat{f}_1^2 \hat{f}_2}}{l_1 \hat{f}_1^2}$$
 and  $\overline{\lambda} = 2 \frac{-\hat{f}_2 + \sqrt{\hat{f}_2^2 + l_2^3 \hat{f}_1^2 \hat{f}_2}}{l_1 \hat{f}_1^2}$ .

When M < 0,  $\hat{A}_0$  has a pair of complex eigenvalues, and its spectral radius is  $\rho_{\hat{A}_0} = \sqrt{-k_1 l_1 \hat{f}_2}$ . Thus, the sufficient condition to  $\rho_{\hat{A}_0} \leqslant \epsilon < 1$ , where  $\epsilon > 0$ ,  $\epsilon \in \mathbb{R}$ , is

$$l_2 < k_2 < l_2 - \frac{\epsilon^2}{\hat{f}_2}.\tag{A2}$$

It is easy to conclude that  $\underline{\lambda} > l_2$ , and further

$$\underline{\lambda} - l_2 + \epsilon^2 / \hat{f}_2 = \frac{(\sqrt{-\hat{f}_2} - \sqrt{-\hat{f}_2 - l_2^3 \hat{f}_1^2})^2}{l_1 \hat{f}_1^2} + \frac{\epsilon^2}{\hat{f}_2} < \frac{1}{l_1 \hat{f}_1^2 \hat{f}_2} (\epsilon^2 (l_2 \underline{f}_{12} + l_1 \hat{f}_2) (l_2 \underline{f}_{12} - (1 + l_2) \hat{f}_2) - (1 - \epsilon^2) \hat{f}_2^2),$$

where  $\underline{f}_{12}$  is the lower bound of  $\hat{f}_1 + \hat{f}_2$ . When  $\hat{\Gamma}_i$  belongs to the convex domain  $D_s$  and when  $\epsilon$  is sufficiently close to 1, inequality  $\underline{\lambda} < l_2 - \epsilon/\hat{f}_2$  holds.

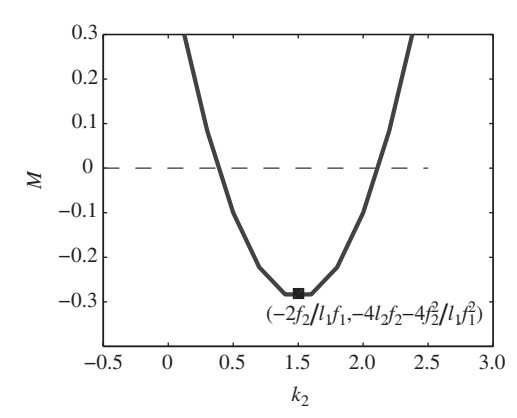


**Figure A1** Values of M as a function of  $k_2$ .

Merging of (A1) and (A2) yields

$$\underline{\lambda} < k_2 < \min\{\overline{\lambda}, l_2 - \epsilon/\hat{f}_2\}.$$
 (A3)

On the other hand, the sufficient condition to M > 0 is

$$k_2 > \overline{\lambda} \text{ or } k_2 < \underline{\lambda}.$$
 (A4)

When M > 0, matrix  $\hat{A}_0$  has a pair of real eigenvalues, and its spectral radius is  $\rho_{\hat{A}_0} = \frac{k_2 l_2 \hat{f}_1 + \sqrt{k_2^2 l_2^2 \hat{f}_1^2 + 4k_1 l_1 \hat{f}_2}}{2}$ Thus, the sufficient condition to  $\rho_{\hat{A}_0} \leqslant \epsilon < 1$  is

$$l_2 < k_2 < \mu, \tag{A5}$$

where  $\mu = \frac{\epsilon^2 + l_2 \hat{f}_2}{\hat{f}_2 + \epsilon l_2 \hat{f}_1}$ . When

$$\hat{f}_2 + l_2^3 \hat{f}_1^2 < 0, \tag{A6}$$

the relationships between  $\underline{\lambda}$ ,  $\overline{\lambda}$ , and  $\mu$  are

$$\underline{\lambda} - \mu < \frac{-2\hat{f}_2}{l_1\hat{f}_1^2} - \frac{\epsilon^2 + l_2\hat{f}_2}{\hat{f}_2 + \epsilon l_2\hat{f}_1} = \frac{1}{l_1\hat{f}_1^2(\hat{f}_2 + \epsilon l_2\hat{f}_1)} (-\hat{f}_2(\hat{f}_2 + l_1l_2\hat{f}_1^2) - (\hat{f}_2 + \epsilon l_2\hat{f}_1)^2) < 0$$

and

$$\overline{\lambda} - \mu = \underline{\lambda} - l_2 - (\mu - l_2) = \frac{(\sqrt{-\hat{f}_2} + \sqrt{-\hat{f}_2 - l_2^3 \hat{f}_1^2})^2}{l_1 \, \hat{f}_2^2} - \frac{\epsilon^2 - \epsilon l_1 \, \hat{f}_1}{\hat{f}_2 + \epsilon l_2 \, \hat{f}_1} > \frac{-2\hat{f}_2 - l_2^3 \hat{f}_1^2}{l_1 \, \hat{f}_2^2} - \frac{\epsilon^2 - \epsilon l_1 \, \hat{f}_1}{\hat{f}_2 + \epsilon l_2 \, \hat{f}_1}.$$

When  $\hat{\Gamma}_i$  belongs to the convex domain  $D_s$  such that  $\hat{f}_1 + \hat{f}_2$  is lower bounded and under condition (A6), inequality  $\bar{\lambda} > \mu$  holds.

Merging (A4) and (A5) according to the relationship  $\underline{\lambda} < \mu < \overline{\lambda}$ , we get

$$l_2 < k_2 < \underline{\lambda}. \tag{A7}$$

When M=0, it is necessarily  $k_2=\overline{\lambda}$  or  $k_2=\underline{\lambda}$ , where  $k_2=\underline{\lambda}$  is a feasible solution in the sense that

Thus, when  $\hat{f}_2 + l_2^3 \hat{f}_1^2 < 0$ , the feasible region of  $k_2$  determined cooperatively by (A3) and (A7) and  $k_2 = \underline{\lambda}$  is

$$l_2 < k_2 < \min\{\overline{\lambda}, l_2 - \epsilon/\hat{f}_2\}. \tag{A8}$$

Case 2: the estimations of  $\hat{f}_1$  and  $\hat{f}_2$  are such that  $.\hat{f}_2 + l_2^3 \hat{f}_1^2 > 0.$ 

In this situation, M is consistently positive, that is, M > 0,  $\forall k_2 \in \mathbb{R}$ , and  $\hat{A}_0$  has a pair of real eigenvalues. The spectral radius of  $\hat{A}_0$  is  $\rho_{\hat{A}_0} = \frac{k_2 l_2 \hat{f}_1 + \sqrt{k_2^2 l_2^2 \hat{f}_1^2 + 4k_1 l_1 \hat{f}_2}}{2}$ . Thus, the feasible region of  $k_2$  when  $\hat{f}_2 + l_2^3 \hat{f}_1^2 > 0$  is

$$l_2 < k_2 < \frac{\epsilon^2 + l_2 \hat{f}_2}{\hat{f}_2 + \epsilon l_2 \hat{f}_1}.$$
(A9)

Case 3: the estimations of  $\hat{f}_1$  and  $\hat{f}_2$  are such that  $\hat{f}_2 + l_2^3 \hat{f}_1^2 = 0$ . M is non-negative. When  $k_2 = \frac{-2\hat{f}_2}{l_1\hat{f}_1^2} = 2l_2$ , M = 0, and the spectral radius is  $\rho_{\hat{A}_0} = \frac{-2l_2^3\hat{f}_1^2}{l_1\hat{f}_1^2} = 2l_2 > 1$ . When  $k_2 \neq 2l_2$ , the sufficient condition to  $\rho_{\hat{A}_0} \leqslant \epsilon < 1$  is  $l_2 < k_2 < \mu$ . Thus, for the special case when  $\hat{f}_2 = -l_2^3\hat{f}_1^2$ , the feasible region is

$$l_2 < k_2 < \mu, \quad k_2 \neq 2l_2.$$
 (A10)

To conclude, according to the estimations of  $\hat{f}_1$  and  $\hat{f}_2$ , there always exist a feasible region for  $k_2$  belonging to one of the three cases such that the eigenvalues of matrix  $\hat{A}_0$  lie within the disc of radius  $\epsilon < 1$ .